

A Letter of Intent to Jefferson Lab PAC26

Measurement of the Target Single-Spin Asymmetry in Quasi-Elastic ${}^3\text{He}^\uparrow(e, e')$

T. Averett

College of William and Mary, Williamsburg, Virginia.

J.-P. Chen

Thomas Jefferson National Accelerator Facility, Newport News, Virginia.

X. Jiang

Rutgers University, Piscataway, New Jersey.

Abstract

We propose to measure the target single-spin asymmetry, A_y , for the neutron using the quasi-elastic ${}^3\text{He}^\uparrow(e, e')$ reaction in Hall A with a vertically polarized ${}^3\text{He}$ target. In the one-photon exchange approximation, A_y is identically zero due to time-reversal invariance. However, it is also sensitive to the two-photon exchange amplitude which can be non-zero and enters A_y through the interference between the one- and two-photon amplitudes. The importance of this two-photon exchange process was emphasized recently as a possible explanation for the discrepancy at large Q^2 between the Rosenbluth separation and polarization transfer techniques used to measure the proton form factor $\mu_p G_E^p/G_M^p$. The discrepancy in the proton form factor data is sensitive to the real part of this interference term, while A_y is sensitive to the imaginary part. For large Q^2 , where the scattering occurs from the partons, the nucleon response during the two-photon process can be calculated using Generalized Parton Distributions (GPD's). Two zeroth moments of the GPD's are needed to describe A_y , but for the neutron, A_y is dominated by just one of these moments, providing clean access to study these GPD's. In this experiment we will measure A_y for the neutron using polarized ${}^3\text{He}$ at the points $Q^2 = 0.9, 1.5, 2.0 \text{ GeV}^2$. The measurement will provide important quantitative information on the two-photon exchange process and access to information about the GPD's at the 10% level.

Contents

1	Introduction	3
2	Physics Motivation	5
2.1	Two-photon-exchange contribution in elastic eN scattering . .	5
2.2	Two-photon contribution to G_E^p/G_M^p	6
2.3	Two-photon contribution to the target single-spin asymmetry A_y	7
2.4	Existing data	8
3	The Proposed Experiment	9
3.1	Kinematics	10
3.2	The luminosity monitors	11
3.3	The vertically polarized ^3He target	12
4	Systematic Uncertainties	13
4.1	Correction on A_y due to target polarization drifts	14
5	Proposed Beam Time	14
6	The Expected Results	14
7	Plans for a Full Proposal	15
8	Summary	15

1 Introduction

For the past forty years, information on nucleon and nuclear structure has been obtained through the study of form factors extracted from elastic electron scattering experiments. Following a well-established formalism, the assumption of the one-photon exchange approximation (Born approximation) allows the interpretation of experimental cross sections in terms of elastic (Dirac and Pauli) form factors. The validity of this approach is based on the assumption that the two-photon-exchange contribution is negligible. As more precision data on cross section and polarization observables becomes available from new facilities, the accuracy of the Born approximation has become one of the major systematic unknowns limiting the interpretation of data.

In the case of the proton form factors, two sets of experimental data consistently yield very different results on the ratio $\mu_p G_{Ep}/G_{Mp}$, as summarized in Figure 1¹. While experiments² using the Rosenbluth method consistently yield $\mu_p G_{Ep}/G_{Mp} \approx 1$ up to $Q^2 \approx 6.0 \text{ GeV}^2$, the Jefferson Lab recoil polarization data^{3,4} demonstrated that G_{Ep}/G_{Mp} decreases quickly as a function of Q^2 . Confirming this discrepancy, preliminary results from the Jefferson Lab Hall A super-Rosenbluth experiment⁵, and the Hall C E94-110 experiment⁶ are in good agreement with the existing cross section data. The existence of this strong discrepancy indicates a fundamental flaw in one of the two ex-

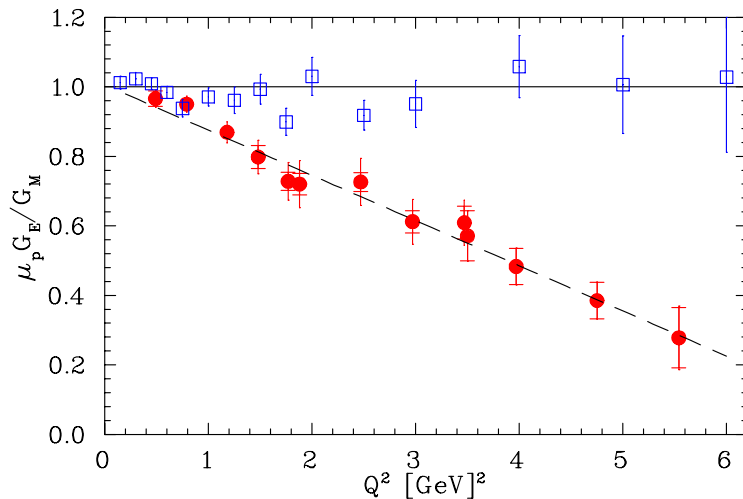


Figure 1: The existing data of $\mu_p G_E/G_M$ for proton¹ from cross section measurements² (open squares) and from recoil polarization measurements^{3,4} (solid circles).

perimental techniques, or a significant systematic error in either the recoil polarization or cross section measurements. The discrepancy in G_{Ep}/G_{Mp} has recently been attributed to a possible failure of the Born approximation at large Q^2 due to two-photon-exchange contributions^{7,8,9}. Calculations show that even a two-photon contribution which is only a few percent of the cross section is enough to bring the results into agreement⁸.

Beyond explaining the form factor discrepancy, a connection was recently made⁹ between the two-photon exchange process and the Generalized Parton Distributions (GPD's)^{10,11} for large Q^2 through the target single spin asymmetry A_y . This asymmetry is measured through inclusive unpolarized electron scattering from a target polarized perpendicular to the scattering plane. It is expected to be zero in the one-photon exchange approximation due to time-reversal invariance, but can receive a non-zero contribution from the interference between the (real) one-photon exchange amplitude and the imaginary part of the two-photon exchange amplitude. For large momentum transfers, the two-photon exchange can be described through the scattering off partons in the nucleon. Its contribution to A_y enters through a weighted integral of the off-forward virtual Compton scattering amplitude with two space-like photons^{12,13}. The physics of the nucleon enters through the hadronic intermediate state (see Figure 2) which can be described as elastic (no nucleon excitation) or inelastic (excited state).

The elastic intermediate state can be exactly calculated¹³ and gives an asymmetry for the proton (neutron) on the order of 1% (-1%). At low Q^2 , the inelastic contributions for the proton could be estimated by inserting specific resonances for the intermediate state. For larger Q^2 , the inelastic contribution to the proton was recently calculated¹³ using deep-inelastic structure functions to describe the intermediate state and gave an asymmetry on the order of 1%. This gives a combined asymmetry for the proton on the order of 2%.

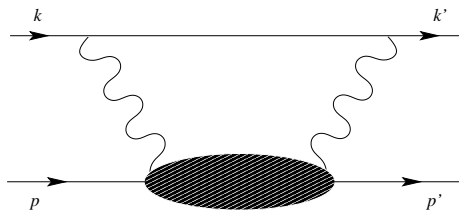


Figure 2: The box diagram of two-photon exchange, the filled ellipse represents the response of the nucleon to the scattering of the virtual photon.

In another approach, it was recently shown that for $Q^2 > 1 \text{ GeV}^2$, the inelastic intermediate state is directly related to the zeroth moments of the GPD's⁹. The neutron is particularly interesting because A_y can be directly related to just one specific moment of the GPD's. A clean measurement of A_y for the neutron is useful for providing additional information about the two-photon exchange process that is important for understanding the form factor data, but is also a powerful experimental tool for accessing information about the GPD's. Because the contribution from the elastic intermediate state is well known, a precise measurement of A_y will be able to provide important information on the response of the nucleon during two-photon exchange. At large enough Q^2 , a precise measurement of A_y will be able to distinguish between GPD models for the inelastic contribution.

Although the importance of observing A_y has been realized for many years, a non-vanishing A_y has never been clearly established in any experiment.

The goal of the experiment proposed here is to make the first measurement of A_y in the quasi-elastic reaction ${}^3\text{He}^\uparrow(e, e')$ at $Q^2 = 0.9, 1.5$ and 2.0 GeV^2 with a statistical uncertainty of 0.2% or below. This precision will allow us to achieve two goals: 1) a clean measurement of the integrated Generalized Parton Distributions 2) quantitative information about the imaginary part of the two-photon exchange process. Together these goals will provide important information about the structure of the nucleon and the physics of the two photon exchange process.

2 Physics Motivation

2.1 Two-photon-exchange contribution in elastic eN scattering

We consider elastic scattering of an electron, l , from a nucleon, N , described by the following kinematics,

$$l(k) + N(p) \rightarrow l(k') + N(p') \quad (1)$$

where the k (k') and p (p') are the four momenta of the incident (scattered) lepton and nucleon respectively. Under Lorentz, parity and charge conjugation invariance, the T -matrix for elastic scattering of two spin-1/2 particles can be expanded in terms of six independent Lorentz structures¹⁸, three of them remain non-zero at the limit of $m_e \rightarrow 0$. Therefore, the T -matrix becomes:

$$T_{h, \lambda'_N \lambda_N} = \frac{e^2}{Q^2} \bar{u}(k', h) \gamma_\mu u(k, h) \times \bar{u}(p', \lambda'_N) \left(\tilde{G}_M \gamma^\mu - \tilde{F}_2 \frac{P^\mu}{M} + \tilde{F}_3 \frac{\gamma \cdot K P^\mu}{M^2} \right) u(p, \lambda_N), \quad (2)$$

where $h = \pm 1/2$ is the electron helicity, λ_N (λ'_N) are the helicities of the incoming (outgoing) nucleon and $K = (k + k')/2$. The quantities \tilde{G}_M , \tilde{F}_2 , \tilde{F}_3 are complex functions of ν and Q^2 , and each contains information about nucleon structure. In the Born approximation, we recover the usual electric and magnetic nucleon form factors as follows:

$$\begin{aligned} \tilde{G}_M^{Born}(\nu, Q^2) &= G_M(Q^2), \\ \tilde{F}_2^{Born}(\nu, Q^2) &= F_2(Q^2), \\ \tilde{F}_3^{Born}(\nu, Q^2) &= 0, \end{aligned} \quad (3)$$

where $F_2 = (G_E - G_M)/(1 + \tau)$ and $\tau = Q^2/4M$. Since \tilde{F}_3 and the phases of \tilde{G}_M and \tilde{F}_2 vanish in the Born approximation, they must originate from processes involving the exchange of at least two photons. We will separate the Born contributions from the multi-photon contributions as follows,

$$\begin{aligned} \tilde{G}_M &= G_M + \delta\tilde{G}_M \\ \tilde{F}_2 &= F_2 + \delta\tilde{F}_2 \end{aligned} \quad (4)$$

We may also use the alternative notation $\tilde{G}_E = G_E + \delta\tilde{G}_E$. Born contributions enter the expression for T at order $O(e^2)$, shown explicitly in Equation 2.

Two photon contributions enter at order $O(e^2)$ relative to the Born contribution which means they contribute to T at order $O(e^4)$. Contributions from multi-photon exchange (more than two) enter beyond $O(e^4)$ and will not be considered here. The box diagram in Figure. 2 represents the most general two-photon exchange process in elastic scattering, with the blob representing the intermediate state of the nucleon.

2.2 Two-photon contribution to G_E^p/G_M^p

Experimentally, two independent methods have been used to determine the ratio of $R = \mu_p G_E^p/G_M^p$ assuming the Born approximation is valid. The first is the Rosenbluth method¹⁷, which uses measurements of the unpolarized cross section:

$$d\sigma_B = C_B(Q^2, \varepsilon) \left[G_M^2(Q^2) + \frac{\varepsilon}{\tau} G_E^2(Q^2) \right], \quad (5)$$

where ε is the photon polarization parameter, and $C_B(Q^2, \varepsilon)$ is a kinematic factor. For a fixed Q^2 , one measures the cross section for different values of ε to determine the form factors G_M and G_E . The second is the polarization method where one measures the ratio of the perpendicular to parallel proton recoil polarization, P_t/P_l , with respect to its momentum direction.

$$\frac{P_t}{P_l} = -\sqrt{\frac{2\varepsilon}{\tau(1+\varepsilon)}} \frac{G_E}{G_M}. \quad (6)$$

As shown in Figure 1, the two sets of experimental data consistently yield very different results. It was pointed out that the discrepancy in G_E/G_M can be explained as a possible failure of the Born approximation when two-photon-exchange contributions are considered^{7,8,9}.

The cross section and the recoil polarization are related to the real part of the two-photon-exchange amplitudes in different ways⁸:

$$\frac{d\sigma}{C_B(\varepsilon, Q^2)} \simeq \frac{|\tilde{G}_M|^2}{\tau} \left\{ \tau + \varepsilon \frac{|\tilde{G}_E|^2}{|\tilde{G}_M|^2} + 2\varepsilon \left(\tau + \frac{|\tilde{G}_E|}{|\tilde{G}_M|} \right) \mathcal{R} \left(\frac{\nu \tilde{F}_3}{M^2 |\tilde{G}_M|} \right) \right\}, \quad (7)$$

$$\frac{P_t}{P_l} \simeq -\sqrt{\frac{2\varepsilon}{\tau(1+\varepsilon)}} \left\{ \frac{|\tilde{G}_E|}{|\tilde{G}_M|} + \left(1 - \frac{2\varepsilon}{1+\varepsilon} \frac{|\tilde{G}_E|}{|\tilde{G}_M|} \right) \mathcal{R} \left(\frac{\nu \tilde{F}_3}{M^2 |\tilde{G}_M|} \right) \right\}, \quad (8)$$

where \mathcal{R} denotes the real part, and $\tilde{G}_E = \tilde{G}_M - (1 + \tau)\tilde{F}_2$.

The size of the real part of the two-photon contribution, $Y_{2\gamma} \equiv \mathcal{R}(\nu \tilde{F}_3/M^2 |\tilde{G}_M|)$, was determined to be at the order of a few percent by fitting the experimental data and assuming the two-photon-exchange contribution alone causes the G_{Ep}/G_{Mp} discrepancy.

A calculation which includes only the elastic intermediate state found that the two-photon-exchange correction has the proper sign and the magnitude to resolve a large part of the discrepancy⁷, as shown in Figure 3.

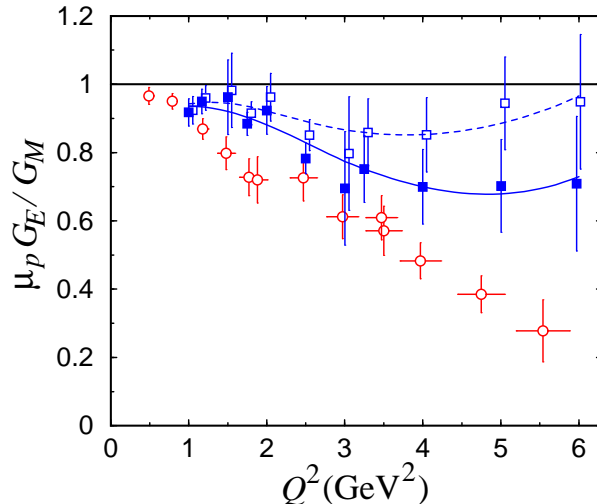


Figure 3: Measured data for the $\mu_p G_E/G_M$ from Rosenbluth separation measurements (open blue squares) and from polarization transfer measurements (open red circles). Neither data set has been corrected for two-photon effects. The solid blue squares show the Rosenbluth data with a two-photon correction applied which includes the elastic intermediate state only.⁷

A more recent calculation⁹ of the two-photon contribution for $Q^2 > 1$ GeV² included both the elastic intermediate state and the inelastic contribution. The inelastic contribution was calculated using a model of the GPD's as input. This calculation brings the data sets into agreement, indicating that the two-photon effects are sufficient to explain the discrepancy.

2.3 Two-photon contribution to the target single-spin asymmetry A_y

An observable which is directly proportional to two-photon exchange is the asymmetry for elastic scattering of an unpolarized electron on a nucleon target polarized normal to the scattering plane (hereafter referred to as vertically polarized).

$$A_y = \frac{\sigma^\uparrow - \sigma^\downarrow}{\sigma^\uparrow + \sigma^\downarrow}, \quad (9)$$

where σ^\uparrow (σ^\downarrow) denotes the cross section for an unpolarized beam and for a nucleon spin parallel (anti-parallel) to the normal polarization vector as defined by the electron scattering plane. As shown by de Rujula *et al.*¹², this asymmetry is related to the absorptive (imaginary) part of the elastic eN scattering amplitude.

Because G_M and G_E are purely real, A_y vanishes in the Born approximation and the leading contribution arises from an interference between the one- and two-photon exchange amplitudes. Neglecting the mass of the electron

and keeping terms which are of order $O(e^4)$, we can write⁹,

$$A_y = \sqrt{\frac{2\varepsilon(1+\varepsilon)}{\tau}} \frac{C_B(\varepsilon, Q^2)}{d\sigma} \times \left\{ -G_M \mathcal{I} \left(\delta\tilde{G}_E + \frac{\nu}{M^2} \tilde{F}_3 \right) + G_E \mathcal{I} \left(\delta\tilde{G}_M + \left(\frac{2\varepsilon}{1+\varepsilon} \right) \frac{\nu}{M^2} \tilde{F}_3 \right) \right\} \quad (10)$$

Y.-C. Chen *et al.*⁹ showed that for $Q^2 > 1 \text{ GeV}^2$, the hard two-photon contributions can be expressed as moments over the GPD's as follows,

$$\begin{aligned} \delta\tilde{G}_M &= C \\ \delta\tilde{G}_E &= -\left(\frac{1+\varepsilon}{2\varepsilon} \right) (A - C) + \sqrt{\frac{1+\varepsilon}{2\varepsilon}} B \\ \tilde{F}_3 &= \frac{M^2}{\nu} \left(\frac{1+\varepsilon}{2\varepsilon} \right) (A - C) \end{aligned} \quad (11)$$

with

$$\begin{aligned} A &= \int_{-1}^1 \frac{dx}{x} K \sum_q e_q^2 (H^q + E^q) \\ B &= \int_{-1}^1 \frac{dx}{x} K \sum_q e_q^2 (H^q - \tau E^q) \\ C &= \int_{-1}^1 \frac{dx}{x} K' \sum_q e_q^2 \tilde{H}^q \end{aligned} \quad (12)$$

where K and K' are kinematic factors and H^q , E^q and \tilde{H}^q are the quark GPD's. Combining Equations 10 and 11, we arrive at the following expression for A_y

$$A_y = \sqrt{\frac{2\varepsilon(1+\varepsilon)}{\tau}} \frac{C_B(\varepsilon, Q^2)}{d\sigma} \{ -G_M \mathcal{I}(B) + G_E \mathcal{I}(A) \} \quad (13)$$

From this expression it is clear that a measurement of A_y will serve as a sensitive test of GPD models. Furthermore, for the neutron, G_E is small which means that the dominant contribution to A_y will come from the term containing $\mathcal{I}(B)$, providing access to one specific moment of the GPD's and making the interpretation cleaner than the proton case where both terms must be included. Using model input for the GPD's, predictions for A_y for the neutron are shown in Figures 4 and 5 for beam energies of 3.6 and 4.8 GeV, respectively.

2.4 Existing data

In the late 1960s, an A_y measurement¹⁴ was among the first generation of SLAC experiments. Using an electron beam with energies of 15 and 18 GeV, A_y , and the induced proton recoil polarization P_y ($A_y = P_y$ by time-reversal invariance), in the elastic ep reaction was observed to be consistent with zero up to $Q^2 = 0.98 \text{ GeV}^2$ within the large experimental uncertainties, as shown in

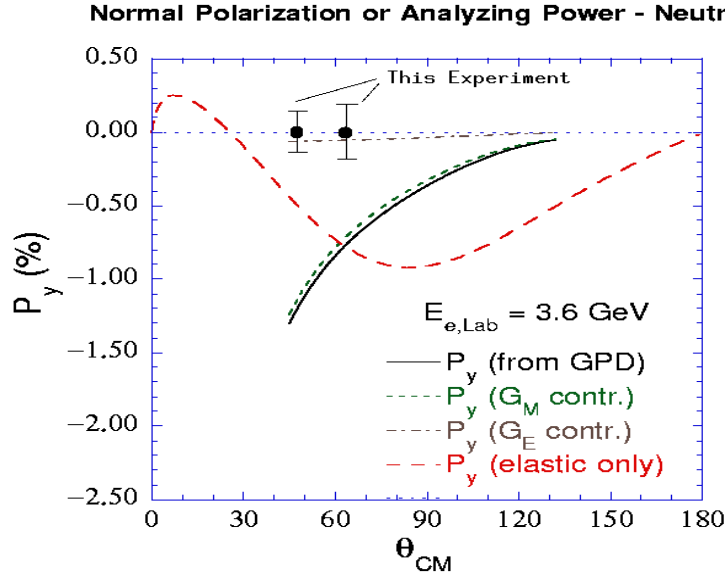


Figure 4: The normal spin asymmetry ($P_y = A_y$) for the neutron for quasi-elastic scattering as a function of the *c.m.* scattering angle for a beam energy of 3.6 GeV. The red dashed curve shows the contribution from the elastic intermediate state. The solid curve shows the contribution from the inelastic intermediate state, calculated using GPD's as input. The total asymmetry is the sum of the solid and dashed curves. The dotted (green) and dot-dash (brown) curves show the individual contributions to the solid curve from the terms containing G_M and G_E respectively. The expected statistical uncertainties from this proposed measurement are shown by the black circles.

Figure 6. However, a rather small A_y is expected ($A_y < 0.5\%$) at the SLAC kinematics¹³ due to the very forward scattering angles, $2.4^\circ < \theta_{lab}^e < 3.2^\circ$ ($13.5^\circ < \theta_{cm}^e < 19.9^\circ$), since A_y is suppressed by a kinematic factor of $\sin \theta_{cm}^e$.

An attempt of measuring A_y in the ${}^3\text{He}(e, e')$ reaction at $Q^2 = 0.1 \text{ GeV}^2$ was also made at NIKHEF¹⁹. Here, A_y was found to be consistent with zero within the large error bars of the experiment at the quasi-elastic peak ($A_y = -0.095 \pm 0.054$) and the Δ -resonance region ($A_y = 0.029 \pm 0.055$).

3 The Proposed Experiment

We plan to measure the target single-spin asymmetry A_y for the neutron in Jefferson Lab Hall A through inclusive quasi-elastic scattering from a vertically polarized ${}^3\text{He}$ target. Measurements will be made at $Q^2 = 0.9, 1.5$ and 2.0 GeV^2 using an unpolarized electron beam. The vertically polarized ${}^3\text{He}$ target will be used in the same configuration as in the approved neutron transversity experiment (E03-004). Two HRS spectrometers on each side of the beam will be used to independently detect the scattered electrons at the same scattering angle. No new equipment is needed for this experiment. The built-in cross-check of $A_y(\theta_e) = -A_y(-\theta_e)$ serves as a clear measure of systematic uncertainties. For some kinematic points, the right HRS will not be

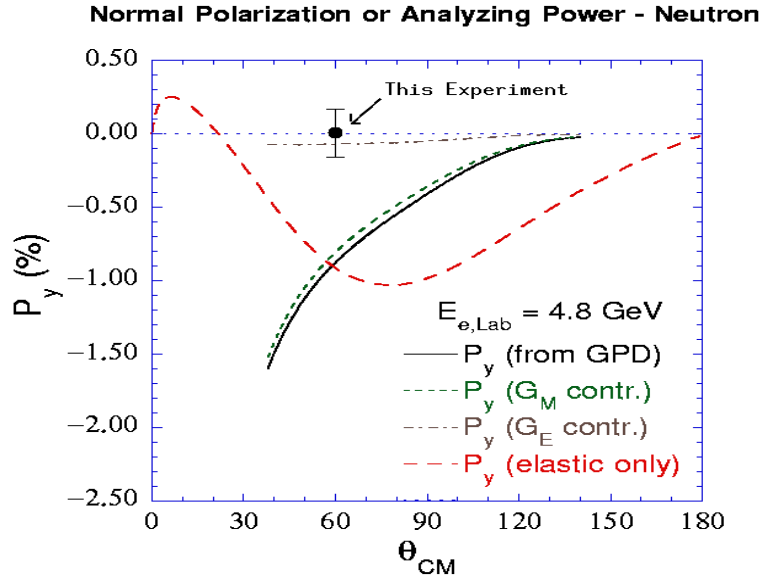


Figure 5: The normal spin asymmetry ($P_y = A_y$) for the neutron for quasi-elastic scattering as a function of the *c.m.* scattering angle for a beam energy of 4.8 GeV. The red dashed curve shows the contribution from the elastic intermediate state. The solid curve shows the contribution from the inelastic intermediate state, calculated using GPD's as input. The total asymmetry is the sum of the solid and dashed curves. The dotted (green) and dot-dash (brown) curves show the individual contributions to the solid curve from the terms containing G_M and G_E respectively. The expected statistical uncertainty from this proposed measurement is shown by the black circle.

able to reach sufficient dipole field for the scattered electron momentum and will be used for background studies and as a luminosity monitor.

Asymmetries will be formed by flipping the polarization direction of the target every few minutes. There should be no correlation between the relative detection efficiency with the target spin direction. The relative beam charge of $Q_{\uparrow}/Q_{\downarrow}$ will be determined by the regular Hall A beam charge monitors. Because we don't care about the beam polarization, we will not have to worry about charge asymmetries in the electron beam. Downstream luminosity monitor units, positioned above and below the beam pipe will count electrons from the target to provide a continuous record of the relative luminosities. The BigBite spectrometer may possibly be used at large angles as luminosity monitor.

3.1 Kinematics

The Q^2 range for this experiment was chosen between 0.9 GeV^2 and 2.0 GeV^2 . The lower limit is chosen to ensure the validity of the GPD interpretation and the upper limit is chosen to minimize inelastic (electron scattering) contributions under the quasi-elastic peak. Guided by theoretical predictions⁹, the largest A_y is expected at center-of-mass angles between $50^\circ \sim 90^\circ$.

Data will be collected at three points in Q^2 , shown in Table 1. The expected rates and total statistical uncertainties for A_y are also listed. Two

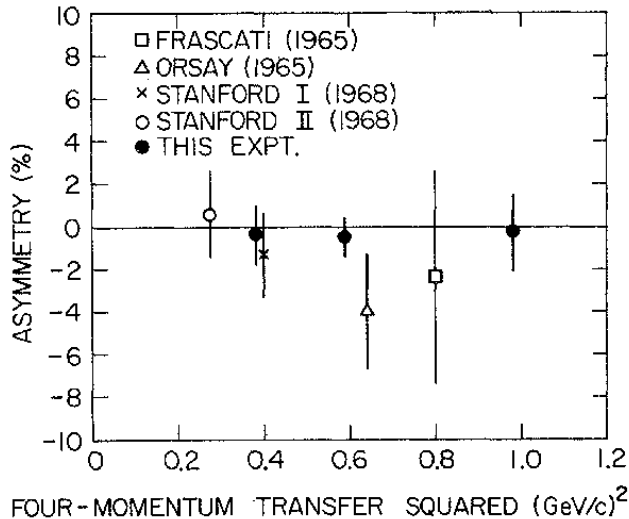


Figure 6: Data from the SLAC A_y measurements¹⁴ referred to as “THIS EXPT.” in the plot. Other data points are from measurements of the induced recoil polarization P_y . Time reversal invariance requires¹² that $P_y = A_y$.

beam energies will be used, $E = 3.6$ GeV and 4.8 GeV. The laboratory scattering angles range from 16.6° to 22.6° , corresponding to center-of-mass scattering angles from 46.5° to 60.9° . The rate and error estimates are based on a 40 cm polarized ^3He target and a $15 \mu\text{A}$ beam with an average target polarization of 0.42. The asymmetry at $E_0 = 4.8$ GeV is shown in Figure 4. For $E_0 = 3.6\text{GeV}$, the behavior of the asymmetry is similar.

E_0 GeV	Q^2 GeV ²	E' GeV	θ_e deg	θ_e^{cm} deg	$^3\text{He}(e, e')$ rate 10 ⁶ per day	Time day	δA_y^n %
3.60	0.93	3.10	16.60	46.5	82	2	0.15
3.60	1.54	2.78	22.60	60.9	8.7	8	0.20
4.80	2.04	3.71	19.50	59.8	4.6	15	0.19

Table 1: Kinematics, count rates, beam time needed and the expected statistical accuracies for each setting.

3.2 The luminosity monitors

Experimentally, the target single-spin asymmetry A_y is only related to the relative yields between target spin up (\uparrow) and spin down (\downarrow) configurations. Knowledge of acceptances, absolute detection efficiencies and absolute luminosities are not necessary. The measured single-spin asymmetry $\mathcal{A}_{measured}$ can be formed from the number of events (N), corrected by the relative lumi-

nosities (\mathcal{L}) corresponding to target spin up and spin down runs.

$$\mathcal{A}_{measured} = \frac{\frac{N_{\uparrow}}{\mathcal{L}_{\uparrow}} - \frac{N_{\downarrow}}{\mathcal{L}_{\downarrow}}}{\frac{N_{\uparrow}}{\mathcal{L}_{\uparrow}} + \frac{N_{\downarrow}}{\mathcal{L}_{\downarrow}}} \quad (14)$$

3.3 The vertically polarized ^3He target

The vertically polarized ^3He target in this proposal is in the same configuration as the approved Hall A neutron transversity experiment (E03-004). The Hall A polarized ^3He target was successfully used for experiments E94-010²⁰ and E95-001²¹ in 1998-1999, and E99-117²² and E97-103²³ in 2001. The polarized ^3He target uses optically pumped rubidium vapor to polarize ^3He nuclei via spin exchange. For a 40 cm long target with target density corresponding to 10 atm at 0°C, average in-beam target polarization is about 42% with beam current of 10-15 μA . Two kinds of polarimetry, NMR and EPR (Electron-Paramagnetic-Resonance), are used to measure the polarization of the target. The uncertainty in the polarization is less than 4%.

The present target configuration, with two sets of Helmholtz coils, can be polarized along any direction in the horizontal plane. Two sets of diode lasers (≈ 100 watts each) and optics are used to polarize the target along the longitudinal and the transverse directions relative to the incident electron momentum. For this experiment (and E03-004), one additional set of coils will be added for the vertical direction. With 3 sets of coils, target polarization along any direction will be possible. The horizontal coils will be oriented to avoid interference with the spectrometer entrances and the beam line. The target cell will be kept in the same shape as the current configuration except for the pull-off tip and the placement inside the scattering chamber. While the target chamber (lower chamber) will be kept unchanged, the pumping chamber (upper chamber) will be tilted 45° to the beam right. The oven for the pumping cell will be modified to be offset with a connection piece to link with the original target ladder. The motion and target ladder system will be kept as it is now with a minor modification of an extension rod to keep the motor and any parts containing magnetic material further away from the target field region. A mirror will be mounted on top of the pumping cell such that the laser light will be reflected into the pumping cell from the top. Another set of mirrors will be placed such that the second laser beam line goes into the pumping cell at 45 degrees off the vertical direction. The mirrors will be chosen to be polarization-preserving mirrors as the ones used in E95-001. A schematic of the target system is shown in Fig. 7 for the side view and the view from beam.

The target spin needs to be flipped frequently to minimize systematic effects. The current NMR system will be modified to sweep the driving frequency through resonance at the Larmor frequency. At this time, the direction of the nucleon spins will flip by 180° relative to the holding field. By inserting (or rotating) a half-wave plate to change the polarization of the laser light,

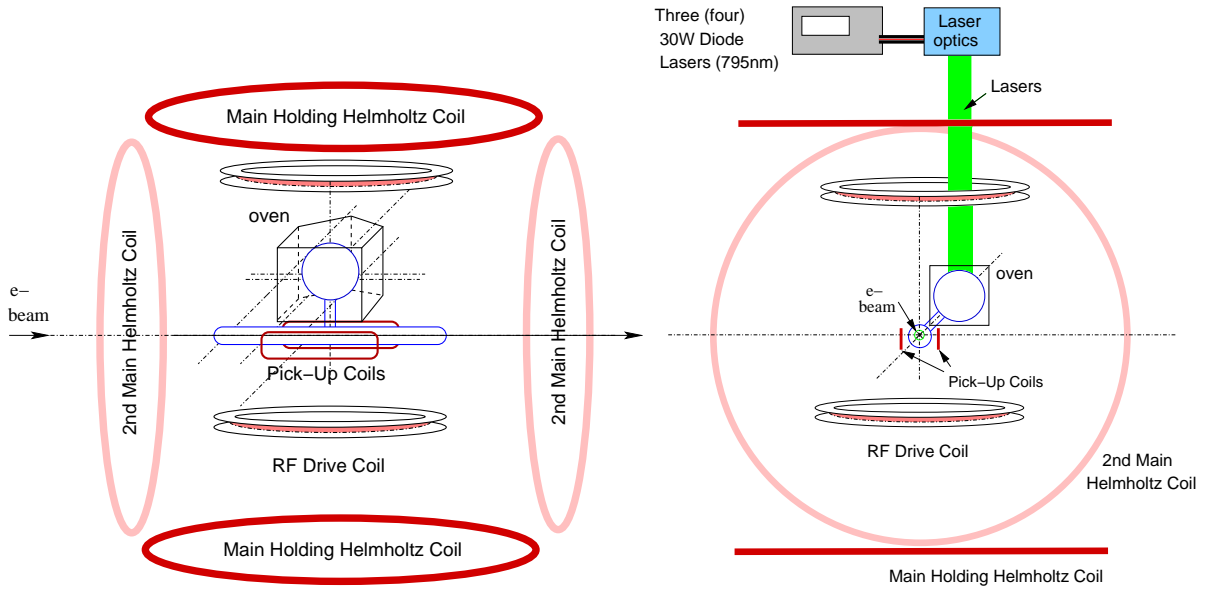


Figure 7: The schematic of the vertically polarized ^3He target, side view (left) and beam view (right).

the target can continue to be polarized in the flipped spin state. It is expected that this spin flip can be accomplished in about 1 minute with minimal loss of polarization. Though not yet fully optimized, the target spin will be flipped about once every hour. Each time the spins are flipped, a measurement of the target polarization is obtained from the NMR system. In addition, the EPR system can be used as needed as a second measurement of the target polarization.

The Jefferson Lab polarized ^3He target system has gone through upgrades and has consistently improved with time. A recent advance in target technology is being explored by the groups of T. Averett *et al.* and the College of William and Mary and G. Cates *et al.* at the University of Virginia. This technology is based on the addition of potassium as an intermediate step in the polarization process²⁴ and is expected to provide a significant improvement in the maximum in-beam target polarization and/or polarization rate. If fruitful, this technology is expected to be integrated into this and other future polarized ^3He experiments.

4 Systematic Uncertainties

Because we are doing quasi-elastic scattering from ^3He , final state interactions must be considered as a possible source of contamination to A_y . In this experiment however, only the scattered electron is detected which means no information about FSI will enter A_y ²⁵. Other possible sources of background come from the ^3He elastic tail and the nucleon inelastic tail, both of which can contribute signal under the quasi-elastic peak. The ^3He elastic contribu-

tion is small at these kinematics and will not contribute significantly to the systematic error. The contribution from the inelastic region may be significant, especially at the largest Q^2 value. A simple estimate of this background indicates that it will be at an acceptable level for this experiment. A more detailed calculation will be performed to confirm this before a full proposal is submitted.

4.1 Correction on A_y due to target polarization drifts

The target polarization between spin up and spin down runs may not be exactly the same. A drift in the target polarization does not cause any single-spin asymmetry itself, but results in a small change which is easy to correct. Assuming the yield is: $\sigma = \sigma_0 + P_T\sigma_1$ for target spin up and spin down, we have: $\sigma_+ = \sigma_0 + P_T\sigma_1$ and $\sigma_- = \sigma_0 - P_T\sigma_1$. The measured asymmetry is:

$$A_0 = \frac{\sigma_+ - \sigma_-}{\sigma_+ + \sigma_-} = P_T \frac{\sigma_1}{\sigma_0}. \quad (15)$$

If during spin down runs the average target polarization changes to $P_T + \delta P_T$, such that $\sigma'_+ = \sigma_0 + P_T\sigma_1$ and $\sigma'_- = \sigma_0 - (P_T + \delta P_T)\sigma_1$, the measured asymmetry changes to:

$$A' = \frac{\sigma'_+ - \sigma'_-}{\sigma'_+ + \sigma'_-} = A_0 \frac{1 + \frac{\delta P_T}{2P_T}}{1 - \frac{\delta P_T}{2P_T} \cdot A_0}. \quad (16)$$

Since $A_0\delta P_T/2P_T \ll 1$, we have:

$$A' \approx A_0 \left(1 + \frac{\delta P_T}{2P_T}\right) \left(1 + \frac{\delta P_T}{2P_T} \cdot A_0\right) \approx A_0 \left(1 + \frac{\delta P_T}{2P_T}\right). \quad (17)$$

As long as the target polarization is measured, the drifts in average polarization between spin up and spin down runs will not cause any significant uncertainty in A_y .

5 Proposed Beam Time

Table 2 outlines the beam time needed to complete this experiment with the statistical uncertainty given above. A total of 600 hours of beam on the polarized target is needed at energies of 3.6 and 4.8 GeV. An additional 96 hours is needed for target spin-flips and polarimetry. Beam polarization is not needed for the A_y measurement, but if available, will us to look for double-spin asymmetries in the same data.

6 The Expected Results

From the measured asymmetry \mathcal{A}_{meas} the physics asymmetry, $A_y^{3\text{He}}$, can be obtained after corrections for the target polarization, P_T , dilution factor, η ,

	Time (hour)
$E_0 = 3.60$ GeV	240
$E_0 = 4.80$ GeV	360
Beam on polarized ^3He target	600
Target overhead, detector checks	96
Total Time Requested	696 (29 days)

Table 2: Possible beam time request for a full proposal at PAC-27.

and radiative effects, R , are applied,

$$A_y {}^3\text{He} = \frac{\mathcal{A}_{meas}}{P_T \eta} R \quad (18)$$

The dilution factor corrects for scattering from unpolarized nitrogen present in the polarized target system and is typically $\eta \sim 0.95$. The neutron asymmetry is extracted by correcting for the neutron and proton polarizations in ^3He according to the formalism of Bissey *et al.*²⁶. The expected statistical uncertainties on A_y are at or below $\delta A_y \sim 0.2\%$ (absolute) and are given in Table 1. Based on the GPD and elastic contributions shown in Figure 4, our measured uncertainty provides a $\sim 10\%$ (relative) measurement of the asymmetry at each of the three values of Q^2 . For comparison of the expected uncertainties with theoretical predictions, see Figures 4 and 5.

7 Plans for a Full Proposal

This Letter of Intent will be developed into a full proposal for PAC-27. A careful study of the background from inelastic scattering will be performed. Studies of frequent target polarization reversal using will be done using the polarized target systems at Jefferson Lab and the College of William and Mary. We are also working with the authors of Ref.⁹ to study the sensitivity of the asymmetry to the choice of GPD model input.

8 Summary

In this Letter of Intent, we outline a measurement of the target single-spin asymmetry A_y in the quasi-elastic elastic $^3\text{He}(e, e')$ reaction in Hall A using a vertically polarized ^3He target. The single-spin asymmetry A_y is sensitive to the imaginary part of the two-photon exchange amplitude and provides clean access to the zeroth moments of the generalized Parton Distributions. In contrast to the proton case, the neutron is particularly useful for this measurement since it is dominated by just one of the moments, and therefore provides cleaner access to the GPD's. The expected statistical uncertainty for A_y will be between 0.15-0.20% and will provide important quantitative in-

formation on the two-photon exchange process and nucleon structure through the GPD's.

References

1. A summary of the existing data can be found in J. Arrington, nucl-ex/0305009.
2. L. Andivahis *et al.*, Phys. Rev. D **50**, 5491 (1994).
3. M.K. Jones *et al.*, Phys. Rev. Lett. **84**, 1398 (2000).
4. O. Gayou *et al.*, Phys. Rev. Lett. **88**, 092301 (2002).
5. Jefferson Lab experiment E01-001, J. Arrington, R.E. Segel, *et al.*
6. M.E. Christy *et al.*, to be submitted to Phys. Rev. C.
7. P.G. Blunden, W. Melnitchouk, J.A.Tjon, nucl-th/0306076 and PRL.
8. P.A.M. Guichon, M. Vanderhaeghen, hep-ph/03060007 and PRL.
9. Y.-C. Chen *et al.*, hep-ph/0403058.
10. X. Ji, Phys. Rev. Lett. **78** (1997) 610.
11. A. Radyushkin, Phys. Lett. B **380** (1996) 417.
12. A. De Rujula, J.M. Kaplan and E. De Rafael, Nucl. Phys. B **53**, 545 (1973).
13. A. Afanasev, I. Akushevich, N.P. Merenkov, hep-ph/0208260.
14. T. Powell *et al.*, Phys. Rev. Lett. **24**, 753 (1970).
15. J. Gunion and L. Stodolsky, Phys. Rev. Lett. **30**, 345 (1973)
16. R. Blankenbecker and J. Gunion, Phys. Rev. D **4**, 718 (1971)
17. M.N. Rosenbluth, Phys. Rev. **79**, 615 (1950).
18. M.L. Goldberger, Y. Nambu and R. Oehme, Ann. of Phys. **2**, 226 (1957).
19. M. C. Harvey, Ph.D. thesis, Hampton University, 2001.
20. M. Amarian *et al.*, Phys. Rev. Lett. **89**, 242301 (2002), and *ibid.*, Phys. Rev. Lett. **92**, 022301 (2004).
21. W. Xu *et al.*, Phys. Rev. Lett. **85**, 2900 (2000), and F. Xiong *et al.*, Phys. Rev. Lett. **87**, 242501 (2001).
22. . X. Zheng *et al.*, Phys. Rev. Lett. **92**, 012004 (2004).
23. JLab E97-103, Spokespersons, T. Averett and W. Korsch; <http://hallaweb.jlab.org/physics/experiments/he3/g2/temp/>
24. E. Babcock *et al.*, Phys. Rev. Lett. **91**, 123003 (2003).
25. A. Afanasev, private communication.
26. F. Bissey *et al.*, Phys. Rev. **C65** (2002) 064317.
27. N. R. Newbury *et al.*, Phys. Rev. Lett. **67**, 3219 (1991).
28. JLab E97-110, Spokespersons, J. P. Chen, A. Deur and F. Garibaldi; <http://hallaweb.jlab.org/physics/experiments/he3/gdh/index.html>.